

## Stress minimization and robust compliance optimization of structures by the level set method

Grégoire Allaire, Frédéric de Gournay, François Jouve

Centre de Mathématiques Appliquées, Ecole Polytechnique, 91128 Palaiseau, France

(gregoire.allaire@polytechnique.fr),

Laboratoire de Mathématiques, Université de Versailles-Saint Quentin en Yvelines, 45 avenue des Etats-Unis,  
78035 Versailles, France (Frederic.de.Gournay@math.uvsq.fr),

Laboratoire J.L.Lions, Université Paris 7 - Denis Diderot, 75252 Paris, France (jouve@math.jussieu.fr)

### 1. Abstract

We discuss two new applications of the level set method in shape and topology optimization of structures in the context of linear elasticity. The first one is the minimization of a stress-based objective function. For such a criterion we compute a shape derivative, as well as a topological derivative, using an adjoint equation. The second one is the so-called worst-case or robust optimal design problem for minimal compliance. In the latter case we seek an optimal shape which minimizes the largest, or worst, compliance when the loads are subject to some unknown perturbations. We first propose a stable algorithm to compute such a worst perturbation (possibly non unique), based on the maximization of a nonlinear energy. Then, in the framework of Hadamard method, we compute the directional shape derivative of this criterion. Since this criterion is usually merely directionally differentiable, we introduce a semidefinite programming approach to select the best descent direction at each step of a gradient method. In the context of the level set method we implement a gradient algorithm for the minimization of these two objective functions and present several numerical examples in 2-d and 3-d.

**2. Keywords:** Topology optimization, level set method, shape derivative.

### 3. Introduction

Since the pioneering papers [2], [3], [8], [10], [11], there has been a burst of publications on the application of the level set method to shape and topology optimization of structures. Most of the recent papers focus on numerical issues for improving the level set method but do not extend so much its range of applicability, focusing merely on compliance minimization which is a notably simpler problem than optimization of a general objective function. The goal of the present paper is, on the contrary, to extend the range of objective functions which are successfully treated by the level set method. More specifically we first consider the case of objective functions depending on the stress tensor [1], then we treat the so-called worst-case or robust optimal design problem for minimal compliance [7]. It clearly demonstrates that the level set method is a versatile tool for structural optimization which can tackle industrial, and not merely academic, problems.

A structure is occupying a bounded domain  $\Omega \subset \mathbb{R}^d$  ( $d = 2$  or  $3$ ) with a boundary made of three disjoint parts

$$\partial\Omega = \Gamma \cup \Gamma_N \cup \Gamma_D, \quad (1)$$

where only  $\Gamma$  is subject to optimization and free to move, while  $\Gamma_N$  and  $\Gamma_D$  are fixed. Homogeneous Neumann boundary condition (no traction) is imposed on the free boundary  $\Gamma$ , a Dirichlet boundary condition on  $\Gamma_D$  and a Neumann boundary condition on  $\Gamma_N$ . All admissible shapes  $\Omega$  are required to be a subset of a fixed working domain  $D$ . The shape  $\Omega$  is occupied by a linear isotropic elastic material with Hooke's law  $A$  defined, for any symmetric matrix  $\xi$ , by

$$A\xi = 2\mu\xi + \lambda(\text{Tr}\xi)I_2,$$

where  $\mu$  and  $\lambda$  are the Lamé moduli of the material. The displacement field  $u$  in  $\Omega$  is the solution of the linearized elasticity system

$$\begin{cases} -\text{div}(Ae(u)) = 0 & \text{in } \Omega \\ u = 0 & \text{on } \Gamma_D \\ (Ae(u))n = g & \text{on } \Gamma_N \\ (Ae(u))n = 0 & \text{on } \Gamma, \end{cases} \quad (2)$$

where  $g$  is a given surface load. For simplicity we do not consider volume forces here although there is again no difficulty to take them into account (see [3]). The objective function is denoted by  $J(\Omega)$  which is implicitly defined in terms of the solution  $u = u(\Omega)$  of (2). We define the set of admissible shapes that must be subset of the working domain  $D$ , of fixed volume  $V$  and satisfying (1)

$$\mathcal{U}_{ad} = \left\{ \Omega \subset D \text{ such that } |\Omega| = V, \Gamma_N \cup \Gamma_D \subset \partial\Omega \right\}. \quad (3)$$

Our model problem of shape optimization is

$$\inf_{\Omega \in \mathcal{U}_{ad}} J(\Omega). \quad (4)$$

In practice we often work with an unconstrained problem. Introducing a Lagrange multiplier  $\ell$ , we consider the Lagrangian minimization

$$\inf_{\Omega \in \mathcal{U}_{ad}} \mathcal{L}(\Omega) = J(\Omega) + \ell|\Omega|. \quad (5)$$

#### 4. Main results

We briefly recall the classical notion of shape derivative, going back to Hadamard, and which is at the root of a gradient method for the minimization of (4). Starting from a smooth and bounded reference shape  $\Omega$ , we consider domains of the type

$$\Omega_\theta = (I_2 + \theta)(\Omega), \quad (6)$$

with  $I_2$  the identity mapping from  $\mathbb{R}^d$  into  $\mathbb{R}^d$  and  $\theta$  a vector field in  $C^1(\mathbb{R}^d, \mathbb{R}^d)$ . It is well known that, for sufficiently small  $\theta$ ,  $(I_2 + \theta)$  is a diffeomorphism in  $\mathbb{R}^d$ . We remark that all admissible domains  $\Omega_\theta$  belong to the class of homotopy of the reference domain  $\Omega$  (it implies that in 2-d the number of connected components of the boundary remains constant). In other words, no change of topology is possible with this method of shape variation.

The shape derivative of  $J(\Omega)$  at  $\Omega$  is defined as the differential at the origin  $\theta = 0$  of the application  $\theta \rightarrow J((I_2 + \theta)(\Omega))$ , i.e.

$$J((I_2 + \theta)(\Omega)) = J(\Omega) + J'(\Omega)(\theta) + o(\theta) \quad \text{with} \quad \lim_{\theta \rightarrow 0} \frac{|o(\theta)|}{\|\theta\|} = 0,$$

where  $J'(\Omega)$  is a continuous linear form on  $C^1(\mathbb{R}^d, \mathbb{R}^d)$ . Because of the constraint (1) on the boundary of all admissible shapes, we assume that all vector fields  $\theta$  vanish on  $\Gamma_N$  and  $\Gamma_D$ , which ensures that  $\Omega_\theta$  satisfy (1).

##### 4.1. Minimum stress optimal design

In this section we consider a stress-based objective function

$$J(\Omega) = \int_{\Omega} k(x) |\sigma|^2 dx, \quad (7)$$

where  $k(x) \in L^\infty(D)$  is a given piecewise smooth non-negative function (a weighting factor that can localize the objective function). More generally we can set

$$J(\Omega) = \int_{\Omega} j(x, \sigma(x)) dx, \quad (8)$$

with a smooth function  $j$ . This allows us, for example, to minimize the equivalent Von Mises stress intensity in  $\Omega$ , or to reach a stress target  $\sigma_0$  (a useful criterion for mechanism design). In both formulas (7) and (8), the stress tensor is

$$\sigma = A e(u)$$

where  $u = u(\Omega)$  is the solution of (2).

In [1] we proved that the shape derivative of (8) is

$$J'(\Omega)(\theta) = \int_{\Gamma} \theta \cdot n \left( j(x, \sigma) + A e(u) \cdot e(p) \right) ds, \quad (9)$$

where  $\sigma = Ae(u)$  and  $p$  is the adjoint state, assumed to be smooth, defined as the solution of

$$\begin{cases} -\operatorname{div}(Ae(p)) &= \operatorname{div}(Aj'(x, \sigma)) & \text{in } \Omega \\ p &= 0 & \text{on } \Gamma_D \\ (Ae(p))n &= -(Aj'(x, \sigma))n & \text{on } \Gamma_N \cup \Gamma, \end{cases} \quad (10)$$

where  $j'$  denotes the partial derivative of  $j(x, \sigma)$  with respect to  $\sigma$ .

#### 4.2. Robust compliance

The notion of worst-case optimisation is an old one, well studied in the literature. In the case of compliance minimization it was called robust or principal compliance and studied in [5]. In the framework of Hadamard method of shape variations it was further explored in [7]. Let us recall its definition in the present context. The compliance for (2) is defined as

$$C_\Omega(g) = \int_{\Gamma_N} g \cdot u \, ds = \max_{v \in V(\Omega)} E_\Omega(v, g), \quad (11)$$

where  $V(\Omega) = \{v : \Omega \rightarrow \mathbb{R}^d \text{ such that } v = 0 \text{ on } \Gamma_D\}$  is the space of kinematically admissible displacements, and  $E_\Omega$  is the elastic energy

$$E_\Omega(v, g) = - \int_{\Omega} Ae(v) \cdot e(v) \, dx + 2 \int_{\Gamma_N} g \cdot v \, ds.$$

Of course, the unique maximizer of the elastic energy in the right hand side of (11) is precisely  $u$ . We assume that the load  $g$  can be decomposed in some known average value  $\bar{g}$  and some unknown perturbation  $\delta g$ , i.e.  $g = \bar{g} + \delta g$ . For a given average load  $\bar{g}$  and a given perturbation threshold  $m \geq 0$ , the robust or worst-case compliance is defined by

$$J(\Omega) = \max_{\|\delta g\| \leq m} C_\Omega(\bar{g} + \delta g). \quad (12)$$

Several possible choices of the norm in the maximization (12) are possible but, for simplicity, we consider

$$\|\delta g\|^2 = \int_{\Gamma_N} |\delta g|^2 \, ds.$$

Other choices could correspond to a localization of the above norm to some subset of  $\Gamma_N$  or to integrate only some components of the vector field  $\delta g$ . Since the robust compliance (12) is defined through two successive maximizations, we can exchange their order and perform explicitly the maximization with respect to  $\delta g$  to obtain a new equivalent formulation

$$J(\Omega) = \max_{v \in V(\Omega)} \left( - \int_{\Omega} Ae(v) \cdot e(v) \, dx + 2 \int_{\Gamma_N} \bar{g} \cdot v \, ds + 2m\|v\| \right). \quad (13)$$

The special case  $\bar{g} = 0$  yields the so-called Auchmuty variational principle for the first (minimal) eigenvalue of a spectral problem where the eigenvalue appears on  $\Gamma_N$  only. As is the case for the first eigenvalue which may admit several independent eigenvectors, the maximization (13) may have several maximizers (corresponding to different worst perturbations  $\delta g$ ). This is at the root of numerical difficulties which are solved in [7]. Furthermore, it implies that the robust compliance (12) is usually not differentiable, but merely directionnaly differentiable (i.e., it admits different derivatives in different directions).

In [7] we proved that the robust compliance (12) admits the following directionnal derivative

$$J'(\Omega)(\theta) = \max_{u \in \mathcal{M}} \int_{\Gamma} \theta \cdot n \left( -Ae(u) \cdot e(u) \right) ds \quad (14)$$

where  $\mathcal{M}$  is the set of maximizers in the definition (13) of  $J(\Omega)$ . In establishing (14) we crucially use the fact that  $\Gamma_N$  is fixed so the norm  $\|v\|$  does not vary with  $\Omega$  satisfying the constraint (1). Our paper [7] also considers more complex cases with bulk forces and design dependent loads.

#### 4.3. Level set algorithm

This section recalls the framework of the level set method as proposed by Osher and Sethian [9]. Consider

a bounded domain  $D \subset \mathbb{R}^d$  in which all admissible shapes  $\Omega$  are included, i.e.  $\Omega \subset D$ . In numerical practice, the domain  $D$  will be uniformly meshed once and for all. We parameterize the boundary of  $\Omega$  by means of a level set function  $\psi$ , defined in  $D$  by

$$\begin{cases} \psi(x) = 0 & \Leftrightarrow x \in \partial\Omega \cap D, \\ \psi(x) < 0 & \Leftrightarrow x \in \Omega, \\ \psi(x) > 0 & \Leftrightarrow x \in (D \setminus \overline{\Omega}). \end{cases} \quad (15)$$

During the optimization process, the shape  $\Omega(t)$  is going to evolve according to a fictitious time parameter  $t \in \mathbb{R}^+$  which corresponds to descent stepping. The evolution of the level set function is governed by the following Hamilton-Jacobi transport equation [9]

$$\frac{\partial\psi}{\partial t} + V|\nabla\psi| = 0 \quad \text{in } D, \quad (16)$$

where  $V(t, x)$  is the normal velocity of the shape's boundary (a scalar function from  $\mathbb{R}^+ \times D$  into  $\mathbb{R}$ ). Equation (16) is simply obtained by differentiating the definition of a level set of  $\psi$ ,  $\psi(t, x(t)) = \text{Cst}$ , and replacing the velocity  $\dot{x}(t)$  by  $Vn$  where the normal  $n$  is equal to  $\nabla\psi/|\nabla\psi|$ . The main advantage of the non-linear equation (16) with respect to a simpler linear transport equation (involving a vector velocity) is that every point  $x \in D$  moves along the normal direction to the level set of  $\psi$  in  $x$ . Recall that, in theory, a tangential velocity does not change the level sets of  $\psi$ , although in practice it yields numerical diffusion which may cause large errors in the position of the boundary  $\partial\Omega$ . Furthermore, (16) takes care of possible self-intersections of the level sets of  $\psi$  and appropriately regularize, or not, possible corners in the shape.

The choice of the normal velocity  $V$  is based on the shape derivative computed in the previous sections for the Lagrangian (5)

$$\mathcal{L}'(\Omega)(\theta) = \int_{\partial\Omega} -V\theta \cdot n \, ds. \quad (17)$$

For the stress-based objective function (8) the integrand  $V$  is given in terms of the state  $u$  and adjoint state  $p$  by

$$V = -\left(j(\sigma) + Ae(u) \cdot e(p) + \ell\right)$$

with  $\ell$ , the Lagrange multiplier for the volume constraint as defined in (5). Remark that  $V$  is defined everywhere in  $D$  and not only on the boundary  $\partial\Omega$ , which is a crucial point for solving (16). We have implicitly chosen a simple normal velocity based on steepest descent,  $\theta = Vn$ . Transporting  $\psi$  by (16) is equivalent to moving the boundary  $\partial\Omega$  (the zero level set of  $\psi$ ) along the descent gradient direction  $-\mathcal{L}'(\Omega)$ . The length of the time interval on which (16) is integrated corresponds to the descent step.

For the robust compliance objective function (12) the choice of the normal velocity  $V$  is more involved. Indeed, remark that the dependence on  $(\theta \cdot n)$  is not fully explicit in the directional shape derivative (14) when the set of maximizers  $\mathcal{M}$  is not reduced to a single maximizer. In such a case, the idea is to take the steepest descent, i.e. to choose  $(\theta \cdot n)$  which minimizes the directional shape derivative (14), subject to a constraint on the magnitude of  $(\theta \cdot n)$ . To implement this idea we add another ingredient which is a regularization of the gradient direction, i.e. we choose a smooth norm to evaluate the constraint on the magnitude of  $(\theta \cdot n)$ . In other words, we change the usual interpretation of the inner product between  $\mathcal{L}'(\Omega)$  and  $\theta$  as the  $L^2(\Gamma)$  scalar product of some integrand with  $W = (\theta \cdot n)$ , and we introduce instead the  $H^1(D)$  scalar product (see [4], [6]). More precisely, we compute the normal velocity  $V$  as the minimizer of

$$\min_{\int_D (|\nabla W|^2 + W^2) dx \leq 1} \left\{ \mathcal{J}(W) = \max_{u \in \mathcal{M}} \int_{\Gamma} W \left( -Ae(u) \cdot e(u) \right) ds \right\} \quad (18)$$

where the function  $\mathcal{J}(W)$  is nothing but the shape derivative  $J'(\Omega)(\theta)$  with the notation  $W = \theta \cdot n$ . The solution of the minimization (18) is actually a low dimensional problem, easy to solve when exploiting the structure of the set  $\mathcal{M}$  (its cardinal is roughly the multiplicity of an eigenvalue, so very often less than 2 in practice). Solving (18) is made by means of a semi-definite programming (SDP) algorithm. We refer to [7] for more details on this issue.

Overall, the level set method allows us to replace the Lagrangian evolution of the boundary  $\partial\Omega$  by the Eulerian solution of the transport equation (16) in the entire fixed domain  $D$ . On the same token, the elasticity equations for the state  $u$  (and for the adjoint state  $p$ ) are extended to the whole domain  $D$  by

using the so-called “ersatz material” approach. It amounts to fill the holes  $D \setminus \Omega$  by a weak phase mimicking void but avoiding the singularity of the stiffness matrix. This is a well-known procedure in topology optimization which we already described in our previous work [3]. In numerical practice, the weak material mimicking holes in  $D \setminus \Omega$  is chosen as  $10^{-3}A$ . The Young modulus of the plain material  $A$  is set to 1 and its Poisson’s ratio is 0.3. For more details on the numerical implementation we refer to our paper [3].

#### 4.4. Numerical results for stress minimization

Our first test case is the well-known L-beam problem, designed to have a re-entrant corner. On Figure 1 we display the boundary conditions and the optimal designs for three objective functions of the type

$$\int_{\Omega} k(x)|\sigma|^{\alpha} dx, \quad \text{with } \alpha = 2, 5, 10.$$

The localizing function  $k(x)$  is equal to 1 everywhere except on a small zone around the point on the right side where the vertical load is applied, where it is set to 0. We use such a localizing function because our goal is to reduce the stress singularity developed in the re-entrant corner and not the one caused by the applied load. The three optimal designs are quite different: for  $\alpha = 10$  we clearly see that the shape is smoothed and “rounded” around the re-entrant corner where a stress singularity can develop.

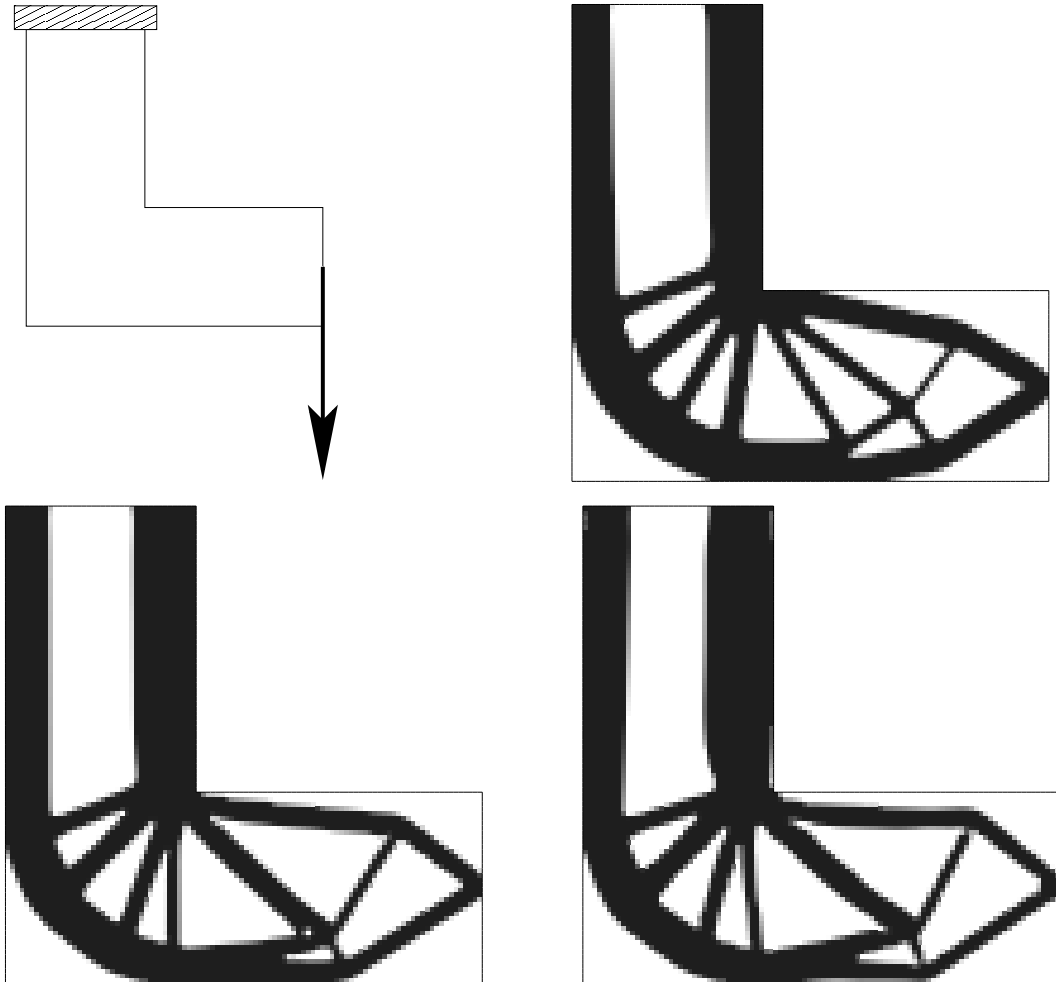


Figure 1: L-beam problem. From top to bottom and left to right: boundary conditions and optimal structures for  $\int_{\Omega} k(x)|\sigma|^{\alpha}$  with  $\alpha = 2, 5$  and  $10$ .

Our second test case is a 3-d optimal mast. The four corners of the bottom of the structure are fixed. Eight vertical loads are applied at the lower corners and the mid-points of the lower edges of the upper

part of the design domain. By symmetry the computation is done on one fourth of the structure. The optimal design for  $\int_{\Omega} |\sigma|^2 dx$  is displayed on Figure 2.

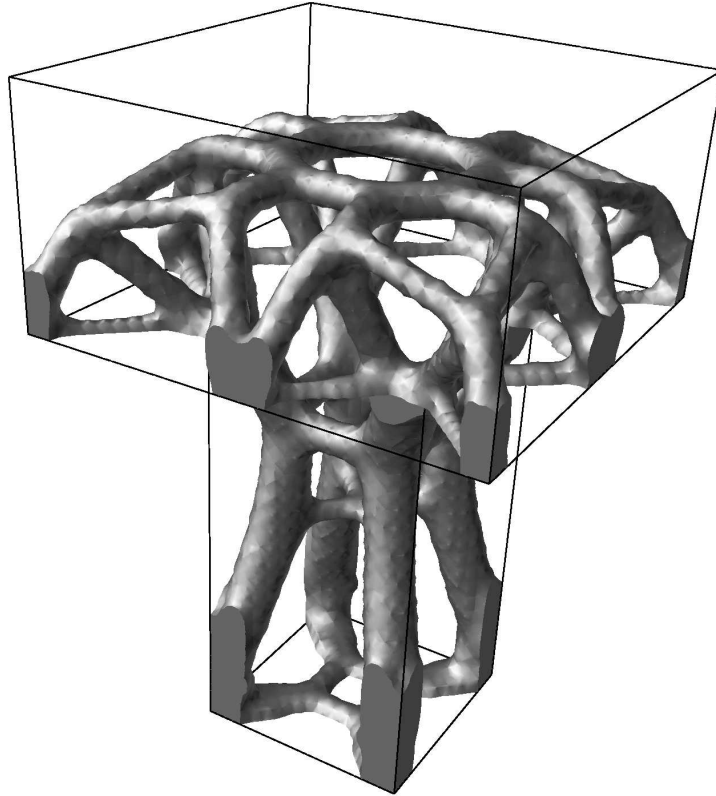


Figure 2: Optimal 3-d mast for  $\int |\sigma|^2$ .

#### 4.5. Numerical results for robust compliance minimization

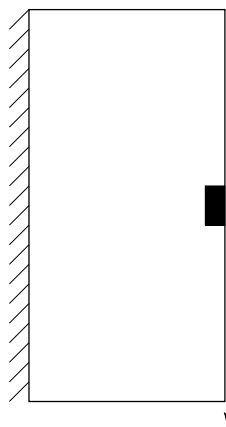


Figure 3: Boundary conditions and loadings for the cantilever test case: the vertical arrow is the average force  $\bar{g}$  while the horizontal perturbations  $\delta g$  are localized in the black box

Our first test case is a cantilever optimization in a  $1 \times 2$  rectangular working domain. The shape is clamped on the left wall and a unit vertical load is applied in the middle of the right wall. Horizontal

perturbations are allowed in a non-optimizable box (the black box of Figure 3) in the middle of the right wall. We perform several runs with an increasing parameter  $m$ , i.e. perturbations of bigger norm are allowed. Different Lagrange multipliers are used so that the optimal shapes have always a volume approximatively equal to 0.2. The other parameters are the same for each run.

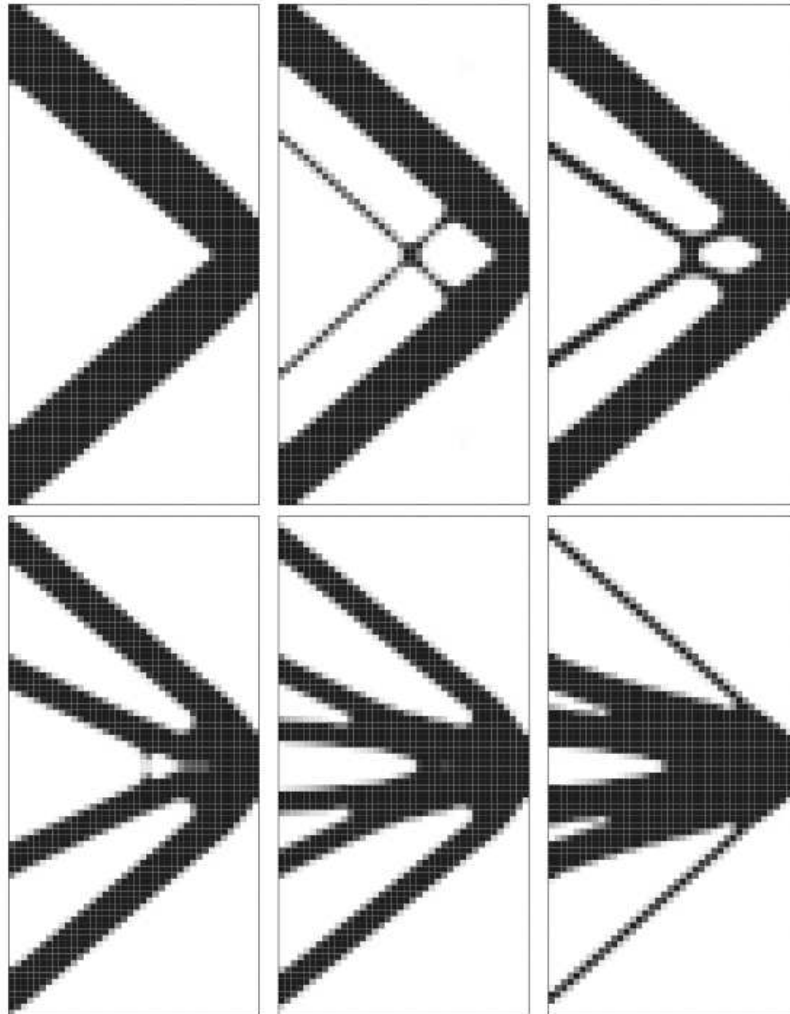


Figure 4: Different values of  $m = 0.1, 0.15, 0.2, 0.3, 0.5, 1$ . in the cantilever problem.

Figure 4 shows the solutions for increasing  $m$  ( $m$  increases from left to right and then from top to bottom). When  $m$  is equal to 0 the robust-compliance problem is a standard compliance problem whose solution is a short cantilever. It can be checked that the upper-left shape is close to this solution ( $m$  is the smallest) and the lower-right shape is closer to a beam ( $m$  is the biggest). When  $m$  is large, the force term is negligible and the problem becomes an eigenvalue problem.

Our second test case is the design of a 3-d chair. The four bottom corners are fixed while the back and the seat of the chair are not subject to optimization and support pressure loads. The pressure applied on the back of the chair is 5 times smaller than the pressure applied on the seat. Perturbations are allowed both on the back and on the seat: they are vertical on the seat and horizontal, perpendicular to the back, 5 times smaller on the back.

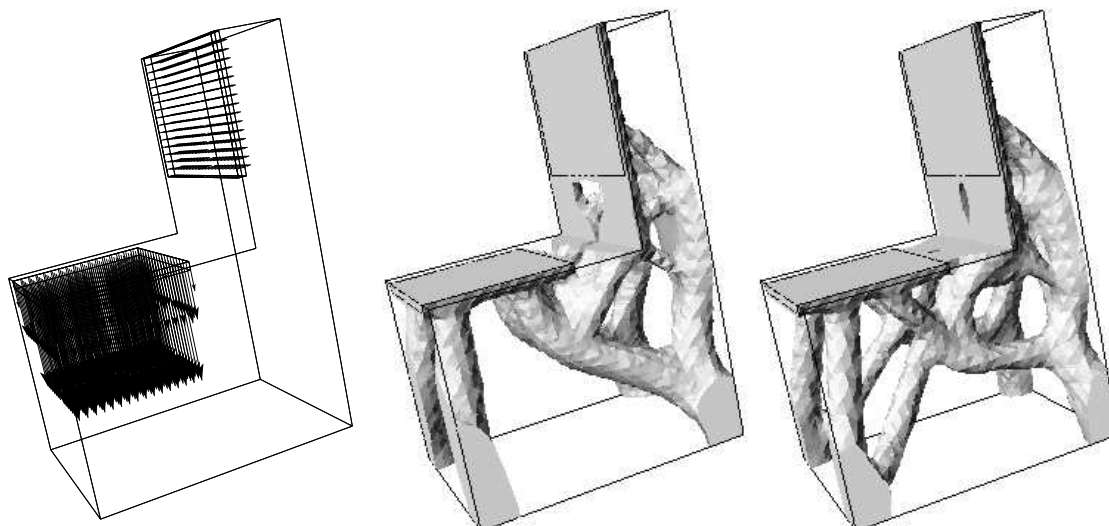


Figure 5: Loading and optimal shape of the chair for  $m = 0$  (left) and  $m = 1$  (right).

Two optimal shapes, for  $m = 0$  and  $m = 1$ , are displayed on Figure 5. The robust-compliance optimal chair has a more complex topology and seems more stable.

## 5. Acknowledgements

G. Allaire is a member of the DEFI project at INRIA Saclay Ile-de-France and is partially supported by the Chair "Mathematical modelling and numerical simulation, F-EADS - Ecole Polytechnique - INRIA".

## 6. References

- [1] G. Allaire, F. Jouve, Minimum stress optimal design with the level set method, *Engineering Analysis with Boundary Elements* **32**, pp.909-918 (2008).
- [2] G. Allaire, F. Jouve, A.-M. Toader, A level set method for shape optimization, *C. R. Acad. Sci. Paris, Série I*, **334**, 1125-1130 (2002).
- [3] G. Allaire, F. Jouve, A.-M. Toader, Structural optimization using sensitivity analysis and a level set method, *J. Comp. Phys.*, **194**, 363–393 (2004).
- [4] M. Burger, A framework for the construction of level set methods for shape optimization and reconstruction, *Interfaces and Free Boundaries*, **5**, pp.301–329 (2003).
- [5] A. Cherkaev and E. Cherkaeva. Principal compliance and robust optimal design, *J. Elasticity*, **72**, pp.71–98 (2003).
- [6] F. de Gournay, Velocity extension for the level-set method and multiple eigenvalues in shape optimization. *SIAM J. on Control and Optim.*, **45**, pp.343–367 (2006).
- [7] F. de Gournay, G. Allaire, F. Jouve, Shape and topology optimization of the robust compliance via the level set method, *COCV* **14**, pp.43-70 (2008).
- [8] S. Osher, F. Santosa, Level set methods for optimization problems involving geometry and constraints: frequencies of a two-density inhomogeneous drum. *J. Comp. Phys.*, **171**, 272–288 (2001).
- [9] S. Osher, J.A. Sethian, Front propagating with curvature dependent speed: algorithms based on Hamilton-Jacobi formulations. *J. Comp. Phys.*, **78**, 12–49 (1988).
- [10] J. Sethian, A. Wiegmann, Structural boundary design via level set and immersed interface methods. *J. Comp. Phys.*, **163**, 489–528 (2000).
- [11] M.Y. Wang, X. Wang, D. Guo, A level set method for structural topology optimization, *Comput. Methods Appl. Mech. Engrg.*, **192**, 227–246 (2003).